Inorg. Chem. **2007**, *46*, 4617–4625

Zero to Three Dimensional Increase of Silver(I) Coordination Assemblies Controlled by Deprotonation of 1,3,5-Tri(2-benzimidazolyl)benzene and Aggregation of Multinuclear Building Units

Xiang-Ping Li,[†] Jian-Yong Zhang,[†] Mei Pan,[†] Sheng-Run Zheng,[†] Yu Liu,[†] and Cheng-Yong Su*[,†,‡]

MOE Laboratory of Bioinorganic and Synthetic Chemistry, State Key Laboratory of Optoelectronic Materials and Technologies, School of Chemistry and Chemical Engineering, Sun Yat-Sen University, Guangzhou 510275, China, and State Key Laboratory of Organometallic Chemistry, Shanghai Institute of Organic Chemistry, Chinese Academy of Sciences, Shanghai 200032, China

Received February 15, 2007

Four Ag(I) complexes of a triangular multidentate ligand 1,3,5-tri(2-benzimidazolyl)benzene (H_3TBimB), namely, $[Ag_2(H_3TBimB)_2](CF_3SO_3)_2$ (**1**), $[Ag_4(HTBimB)_2]_n$ (**2**), $[Ag_9(HTBimB)_4(TAZ)]_n$ (HTAZ = 1,2,4-triazole) (**3**), and $[Ag_{17}(TBimB)_5(HTBimB)(H_2O)_5]_n \cdot nH_2O$ (**4**), have been synthesized at different pH values adjusted by addition of $NH_3 \cdot H_2O$ under solvothermal conditions and characterized by X-ray single-crystal diffraction. Complex **1** shows an M_2L_2 dimeric structure, **2** displays a one-dimensional chain containing M_4L_2 basic units, **3** is a two-dimensional network built up from an M_9L_4 subunit, and **4** exhibits a three-dimensional framework generated by an $M_{17}L_6$ motif. Dimensional increase in complexes **1**–**4** was caused by deprotonation of the H_3TBimB ligand, thus offering more coordinating donors and resulting in aggregation of oligomeric Ag(I) building units. In the cases of complexes **3** and **4**, TAZ or H_2O molecules serve as auxiliary ligands to complete the coordination geometry of the Ag(I) ions wherever necessary. The photoluminescent properties of the ligand H_3TBimB and the complexes **1**–**3** have been investigated.

Introduction

There has been rapidly growing interest in the design, synthesis, and characterization of novel coordination polymers,[1,2] not only due to their fascinating structures and topologies but also because of their potential optical, electronic, and magnetic properties.[3] It is well-known that solvothermal (including hydrothermal) reactions are widely used to prepare coordination polymers. However, the control of products in solvothermal reactions is still an arduous challenge to chemists, since many reaction variables can affect the final products.[4] The pH value is one of the important factors that can significantly influence the structural dimensionalities of the coordination polymers assembled under solvothermal conditions,[5,6] and so far, a number of investigations based on the carboxylic acid ligands[5] have

* To whom correspondence should be addressed. E-mail: cesscy@mail.sysu.edu.cn.
† Sun Yat-Sen University.
‡ Chinese Academy of Sciences.

(1) (a) Carlucci, L.; Ciani, J.; Proserpio, D. M. *Coord. Chem. Rev.* **2003**, *246*, 247. (b) Batten, S. R.; Robson, R. *Angew. Chem., Int. Ed.* **1998**, *37*, 1460. (c) Zaworotko, M. *Chem. Commun.* **2001**, 1. (d) Batten, S. R. *CrystEngComm* **2001**, *3*, 67. (e) Delgado-Friedrichs, O.; Foster, M. D.; O' Keeffe, M.; Proserpio, D. M.; Treacy, M. M. J.; Yaghi, O. M. *J. Solid State Chem.* **2005**, *178*, 2533. (f) Baburin, I. A.; Blatov, V. A.; Carlucci, L.; Ciani, G.; Proserpio, D. M. *J. Solid State Chem.* **2005**, *178*, 2471. (g) James, S. L. *Chem. Soc. Rev.* **2003**, *32*, 276.

(2) (a) Eddaoudi, M.; Moler, D. B.; Li, H. L.; Chen, B. L.; Reineke, T. M.; O' Keeffe, M.; Yaghi, O. M. *Acc. Chem. Res.* **2001**, *34*, 319. (b) Rosi, N. L; Kim, J.; Eddaoudi, M.; Chen, B.; O'Keeffe, M.; Yaghi, O. M. *J. Am. Chem. Soc.* **2005**, *127*, 1504. (c) Ockwig, N. W.; Delgado-Friedrichs, O.; O' Keeffe, M.; Yaghi, O. M. *Acc. Chem. Res.* **2005**, *38*, 176. (d) Khlobystov, A. N.; Blake, A. J.; Champness, N. R.; Lemenovskii, D. A.; Majouga, A. G.; Zyk, N. V.; Schröder, M. *Coord. Chem. Rev.* **2001**, *222*, 155. (e) Hill, R. J.; Long, D.-L.; Champness, N. R.; Hubberstey, P.; Schröder, M. *Acc. Chem. Res.* **2005**, *38*, 337.

(3) (a) Chen, C.-L.; Kang, B.-S.; Su, C.-Y. *Aust. J. Chem.* **2006**, *59*, 3. (b) Janiak, C. *Dalton Trans.* **2003**, 2781. (c) Kitagawa, S.; Kitaura, R.; Noro, S. *Angew. Chem., Int. Ed.* **2004**, *43*, 2334. (d) Moulton, B.; Zaworotko, M. J. *Chem. Rev.* **2001**, *101*, 1629. (e) Inoue, K.; Imai, H.; Ghalsasi, P. S.; Kikuchi, K.; Ohba, M.; Okawa, H.; Yakhmi, J. V. *Angew. Chem., Int. Ed.* **2001**, *40*, 4242. (f) Ramón, J.; Mascarós, G.; Dunbar, K. R. *Angew. Chem., Int. Ed.* **2003**, *42*, 2289. (g) Hong, M. *Cryst. Growth Des.* **2007**, *7*, 10. (h) Hagrman, P. J.; Hagrman, D.; Zubieta, J. *Angew. Chem., Int. Ed.* **1999**, *38*, 2638.

(4) (a) Lu, W.-G.; Jiang, L.; Feng, X.-L.; Lu, T.-B. *Cryst. Growth Des.* **2006**, *6*, 564. (b) Huang, X.-C.; Zhang, J.-P.; Chen, X.-M. *J. Am. Chem. Soc.* **2004**, *126*, 13218. (c) Wang, Y.-L.; Yuan, D.-Q.; Bi, W.-H.; Li, X.; Li, X.-J.; Li, F.; Cao, R. *Cryst. Growth Des.* **2005**, *5*, 1849.

10.1021/ic070309k CCC: $37.00
Published on Web 04/28/2007

been carried out. By contrast, the studies on the neutral ligands containing NH groups remain relatively less explored.[6]

Similar to the neutral ligands 2,2′-bibenzimidazole[6a] and tris(2-benzimidazolylmethyl)amine (H_3ntb),[6b] the rigid triangular ligand 1,3,5-tri(2-benzimidazolyl)benzene (H_3TBimB) contains multiple amine sites with the possibility of reversible deprotonation. Therefore, this ligand can provide versatile coordination modes to interact with transition metal ions: nondeprotonated (H_3TBimB), monodeprotonated (monoanion, H_2TBimB^-), dideprotonated (dianion, $HTBimB^{2-}$), and trideprotonated (trianion, $TBimB^{3-}$), giving rise to three, four, five, and six potential nitrogen donors, respectively. As a consequence, through stepwise deprotonation of the H_3TBimB ligand, systematically diversified supramolecular architectures could be expected from the above varied kinds of multidentate forms controlled by adjusting the reaction basicity. In this Article we report four Ag(I) complexes, $[Ag_2(H_3TBimB)_2](CF_3SO_3)_2$ (**1**), $[Ag_4(HTBimB)_2]_n$ (**2**), $[Ag_9(HTBimB)_4(TAZ)]_n$ (**3**), and $[Ag_{17}(TBimB)_5(HTBimB)(H_2O)_5]_n \cdot nH_2O$ (**4**), obtained from solvothermal reactions of the $AgCF_3SO_3$ and H_3TBimB ligands at different basic conditions.

Experimental Section

All chemicals were commercial products of reagent grade and were used without further purification. The ligand H_3TBimB was prepared according to the literature method.[7] The C, H, and N elemental analyses were performed on a Perkin-Elmer 240 elemental analyzer. IR spectra were recorded on a Bruker Tensor 27 FTIR spectrophotometer using KBr discs in the 4000−400 cm^{-1} region. Photoluminescence was measured on a FLS920 spectrometer. Thermogravimetric analysis was carried out on a NETZSCH TG 209 instrument under 1 atm pressure at a heating rate of 10 °C min^{-1} by heating the sample from 23 to 700 °C. The XRD patterns were recorded on a D/Max-IIIA diffractometer with graphite monochromatized Cu Kα radiation (λ = 1.5418 Å).

$[Ag(H_3TBimB)](CF_3SO_3)$ (1). A mixture of H_3TBimB (0.05 mmol, 0.021 g), $AgCF_3SO_3$ (0.1 mmol, 0.026 g), ethanol (5 mL), and H_2O (10 mL) at pH = 8 was heated in a 20 mL Teflon autoclave at 130 °C for 2 days and then cooled to room temperature at the rate of 5 °C/h. The colorless crystals of hexagonal platelets were separated by filtration. Yield: 70%. Anal. Calcd for $C_{56}H_{36}Ag_2F_6N_{12}O_6S_2$: C, 49.21; H, 2.65; N, 12.30%. Found: C, 49.48; H, 2.61; N, 13.13%. IR (KBr, cm^{-1}): 3436 (br, ν_{N-H}), 3221(m), 1628(w, $\nu_{C=C,C=N}$), 1532(w), 1441(m, $\nu_{C=C,C=N}$), 1252(s, $\nu_{S=O}$), 1177(w), 1029(m, $\nu_{S=O}$), 744(m), 638(m). The same product was obtained when changing the reagents ratio and elevating the temperature from 130 to 160 °C.

$[Ag_4(HTBimB)_2]_n$ (2). A mixture of H_3TBimB (0.1 mmol, 0.042 g), $AgCF_3SO_3$ (0.15 mmol, 0.039 g), and $NH_3 \cdot H_2O$ (15 mL) was heated in a 20 mL Teflon autoclave at 140 °C for 80 h and then cooled to room temperature at the rate of 3 °C/h. The product of reddish strips was separated by filtration. Yield: 90%. IR (KBr, cm^{-1}): 3433(br, ν_{N-H}), 3057(w), 1608(m, $\nu_{C=C,C=N}$), 1412(s, $\nu_{C=C,C=N}$), 1284(m), 1151(w), 1086(w), 939(m), 741(s), 647(w).

$[Ag_9(HTBimB)_4(TAZ)]_n$ (3). A mixture of H_3TBimB (0.1 mmol, 0.042 g), $AgCF_3SO_3$ (0.15 mmol, 0.039 g), 1,2,4-triazole (0.1 mmol, 0.069 g), and $NH_3 \cdot H_2O$ (15 mL) was heated in a 20 mL Teflon autoclave at 160 °C for 3 d and then cooled to room temperature at the rate of 5 °C/h. The colorless hexagonal platelets were obtained. Yield: 60%. IR (KBr, cm^{-1}) 3445(br, ν_{N-H}), 3054(w), 1600(m, $\nu_{C=C,C=N}$), 1417(s), 1278(s), 1213(w), 1113(w), 1033(w), 884(m), 746(m), 505(m).

$[Ag_{17}(TBimB)_5(HTBimB)(H_2O)_5]_n \cdot nH_2O$ (4). A mixture of H_3TBimB (0.05 mmol, 0.021 g), $AgCF_3SO_3$ (0.1 mmol, 0.026 g), Bu_4NBr (0.06 mmol, 0.01 g), and $NH_3 \cdot H_2O$ (15 mL) was heated in a 20 mL Teflon autoclave at 160 °C for 80 h and then cooled to room temperature at the rate of 5 °C/h. The reddish products were obtained. Yield: 30%. IR (KBr, cm^{-1}): 3405(m, $\nu_{N-H,O-H}$), 3106(m), 1605(m, $\nu_{C=C,C=N}$), 1528(w), 1488(w), 1409(s), 1398(m), 1277(m), 1228(w), 1150(w), 1111(w), 1035(w), 882(w), 850(w), 744(s), 701(w).

X-ray Structure Analyses. X-ray diffraction data were collected on a Siemens P4 four-cycle diffractometer for **1** and a Bruker Smart 1000 CCD diffractometer for **2**−**4** with graphite-monochromated Mo Kα radiation (λ = 0.710 73 Å) at room temperature. The Siemens P4 diffractometer was run using the CAD4 Express Software,[8] and the data were processed by the program XCAD-4.[9] The Bruker Smart 1000 CCD diffractometer was run using the program SMART,[10] and the data were processed by SAINT+.[11] Absorption corrections were applied for complexes **2**−**4** with the SADABS program.[12] The structures were solved by the direct method (SHELXS) and refined by the full-matrix least-squares method against F_o^2 using SHELXTL software.[13] The coordinates of the non-hydrogen atoms were refined anisotropically. All hydrogen atoms were introduced in calculated positions except those for water molecules and refined with fixed geometry with respect to their carrier atoms. Crystallographic data and other pertinent information for **1**−**4** are summarized in Table 1. Selected bond lengths and bond angles are listed in Table 2.

Results and Discussion

The ligand H_3TBimB features triangular multidentate character that possesses three imine N atoms and three amine NH groups. The three imine N atoms can act as coordination donors directly, while the three amine NH groups can behave as hydrogen bond donors (H-D). These NH groups can also be partially or fully deprotonated to generate H_2TBimB^-, $HTBimB^{2-}$, or $TBimB^{3-}$ anionic forms at different pH

(5) (a) Wang, C.-C.; Yang, C.-H.; Lee, G.-H. *Eur. J. Inorg. Chem.* **2006**, 820. (b) Zhou, Y.-F.; Lou, B.-Y.; Yuan, D.-Q.; Xu, Y.-Q.; Jiang, F.-L.; Hong, M.-C. *Inorg. Chim. Acta.* **2005**, *358*, 3057. (c) Groves, J. A.; Wright, P. A.; Lightfoot, P. *Dalton. Trans.* **2005**, *11*, 2007. (d) Ou, G.-C.; Su, C.-Y.; Yao, J.-H.; Lu, T.-B. *Inorg. Chem. Commun.* **2005**, *8*, 421. (e) Zheng, Y.-Z.; Tong, M.-L.; Chen, X.-M. *New J. Chem.* **2004**, *28*, 1412. (f) Sun, H.-L.; Ye, C.-H.; Wang, X.-Y.; Li, J.-R.; Gao, S.; Yu, K.-B. *J. Mol. Struct.* **2004**, *702*, 77. (g) Pan, L.; T. Frydel.; M. B. Sander.; Huang, X.; Li, J. *Inorg. Chem.* **2001**, *40*, 1271. (h) Pan, L.; Huang, X.; Li, J. *J. Solid. State. Chem.* **2000**, *152*, 236.

(6) (a) Akutagawa, T.; Saito, G.; Kusunoki, M.; Sakaguchi, K. *Bull. Chem. Soc. Jpn.* **1996**, *69*, 2487. (b) Moon, D.; Lah, M. S. *Inorg. Chem.* **2002**, *41*, 4708. (c) Chen, X.-M.; Tong, M.-L. *Acc. Chem. Res.* **2007**, *40*, 162.

(7) Hiraoka, S.; Yi, T.; Shiro, M.; Shionoya, M. *J. Am. Chem. Soc.* **2002**, *124*, 14510.

(8) *CAD4 Express Software*; Enraf-Nonius: Delft, The Netherlands, 1994.

(9) Harms, K.; Wocadlo, S. *XCAD-4. Program for Processing CAD-4 Diffractometer Data*; University of Marburg: Marburg, Germany, 1995.

(10) *SMART*, version 5.0; Bruker AXS: Madison, WI, 1998.

(11) *SAINT+*, version 6.0; Bruker AXS: Madison, WI, 1999.

(12) *SADABS*, version 2.05; Bruker Nonius area detector scaling and absorption correction; Bruker AXS: Madison, WI, 1998.

(13) Sheldrick, G. M. *SHELX 97;* program for crystal structure solution and refinement; University of Göttingen: Göttingen, Germany, 1997.

Table 1. Crystal Data and Structure Refinement Parameters for Complexes **1**−**4**

	1	**2**	**3**	**4**
empirical formula	$C_{56}H_{36}Ag_2F_6N_{12}O_6S_2$	$C_{27}H_{17}Ag_2N_6$	$C_{110}H_{66}Ag_9N_{27}$	$C_{324}H_{206}Ag_{34}N_{72}O_{12}$
fw	1366.83	640.20	2736.73	8967.19
crystal syst	triclinic	orthorhombic	orthorhombic	monoclinic
space group	$P\bar{1}$	*Fdd*2	*Pbcn*	*P*2(1)/*n*
a (Å)	9.4460(19)	30.350	15.153(9)	13.8011(8)
b (Å)	11.592(2)	34.864	25.681(14)	25.0364(16)
c (Å)	12.042(2)	8.840	24.530(14)	22.6040(15)
α (deg)	87.87(3)	90	90	90.00
β (deg)	85.77(3)	90	90	93.485(4)
γ (deg)	83.79(3)	90	90	90.00
V (Å^3)	1306.7(5)	9354(3)	9545(9)	7795.9(8)
Z	1	16	4	1
D_{calc} (g cm^{-3})	1.737	1.818	1.904	1.910
μ (mm^{-1})	0.918	1.703	1.872	2.149
T (K)	293(2)	293(2)	293(2)	293(2)
R_1	0.0489	0.0357	0.0864	0.0689
wR2	0.1258	0.0684	0.1355	0.1331

Table 2. Selected Bond Lengths (Å) and Angles (deg) for Complexes **1**−**4**

		Complex **1**			
Ag(1)−N(5)	2.120(4)	N(2)−Ag(1A)	2.122(4)	Ag(1)−N(2A)	2.122(4)
N(5)−Ag(1)−N(2A)	169.11(13)				
		Complex **2**			
Ag1−N1	2.048(4)	Ag1−N4	2.058(4)	Ag2−N5	2.070(4)
Ag2−N3	2.079(4)	N1−Ag1−N4	176.11(17)	N5−Ag2−N3	176.25(17)
		Complex **3**			
Ag1−N	7 2.091(9)	Ag1−N1	2.093(9)	Ag2−N5	2.036(11)
Ag2−N9	2.045(10)	Ag3−N6	2.075(9)	Ag3−N2	2.094(10)
Ag4−N10	2.062(10)	Ag4−N10	2.062(10)	Ag5−N4	2.233(10)
Ag5−N4	2.233(10)	Ag5−N13	2.243(16)	Ag6−N8	2.086(10)
Ag6−N8	2.086(10)	N7−Ag1−N1	170.2(4)	N5−Ag2−N9	171.6(4)
N6−Ag3−N2	164.9(4)	N10−Ag4−N10	171.2(6)	N4−Ag5−N4	128.3(5)
N4−Ag5−N13	115.8(3)	N4−Ag5−N13	115.8(3)	N8−Ag6−N8	180.0(8)
		Complex **4**			
Ag1−N1	2.226(8)	Ag1−N7	2.265(9)	Ag1−N13	2.313(8)
Ag2−N9	2.205(9)	Ag2−N17	2.229(9)	Ag2−O2	2.49(3)
Ag3−N6	2.199(9)	Ag3−N15	2.275(9)	Ag3−O1	2.532(15)
Ag4−N3	2.124(9)	Ag4−N11	2.131(8)	Ag5−N2	2.115(9)
Ag5−N2	2.115(9)	Ag6−N10	2.082(8)	Ag6−N14	2.083(7)
Ag7−N16	2.099(10)	Ag7−N12	2.122(9)	Ag8−N4	2.089(9)
Ag8−N18	2.103(8)	Ag9−N5	2.056(8)	Ag9−O4	2.110(11)
N1−Ag1−N7	129.1(3)	N1−Ag1−N13	130.4(3)	N7−Ag1−N13	98.9(3)
N9−Ag2−N17	114.8(3)	N9−Ag2−O2	118.5(8)	N17−Ag2−O2	107.1(9)
N6−Ag3−N15	114.8(3)	N6−Ag3−O1	135.7(5)	N15−Ag3−O1	106.1(5)
N3−Ag4−N11	163.9(3)	N2−Ag54−N2	180.0(6)	N10−Ag6−N14	177.3(3)
N16−Ag7−N12	170.6(3)	N4−Ag8−N18	170.5(3)	N5−Ag9−O4	175.1(4)

conditions as shown in Scheme 1. Once the NH groups are deprotonated, the resulting N atoms become potential coordination donors. On the other hand, all these imine N atoms and deprotonated amine N atoms are potential hydrogen bond acceptors (H-A) if not interacting with the metal ions.

Complexes **1**−**4** were prepared under varied solvothermal reaction conditions from H_3TBimB and $AgCF_3SO_3$. Complex **1** was obtained in a mixture of ethanol and H_2O with a volume ratio of 1:2. The change of the metal-to-ligand ratio and temperature between 130 and 160 °C had no influence on the products; however, reaction in pure water could not give the same complex. Complex **2** was synthesized in a basic solvothermal condition in the presence of 25% ammonia with high yield. Addition of ethanol or too much water caused a failure to give pure product. Complex **3** was formed in a similar reaction condition to that of complex **2**, but the second ligand 1,2,4-triazole (HTAZ) was added to affect the assembly process. In comparison, addition of Bu_4NBr instead of HTAZ in the same reaction system led to formation of complex **4**. These results indicate that the formation of complexes **1**−**4** is considerably influenced by the nature of the solvent system, and the auxiliary ligands also play important roles besides the basicity. All the complexes are insoluble in water and common organic solvents such as ethanol, methanol, acetone, dichloromethane, chloroform, toluene, DMSO, and DMF.

Crystal Structure. $[Ag_2(H_3TBimB)_2](CF_3SO_3)_2$. Single-crystal X-ray analysis reveals that **1** is a dinuclear structure. The coordination environments of the Ag(I) atoms are shown in Figure 1. Each H_3TBimB ligand binds to two Ag(I) atoms and in turn each Ag(I) atom coordinates with two imine N atoms from two different H_3TBimB ligands, thus resulting in a bent (∠N−Ag−N, 169.11(13)°) coordination geometry. The third imine N atom of each ligand is kept uncoordinated. Two central benzene rings are parallel with the centroid−centroid distance between two rings being 3.88(5) Å. Three benzimidazole rings are not coplanar with respect to the

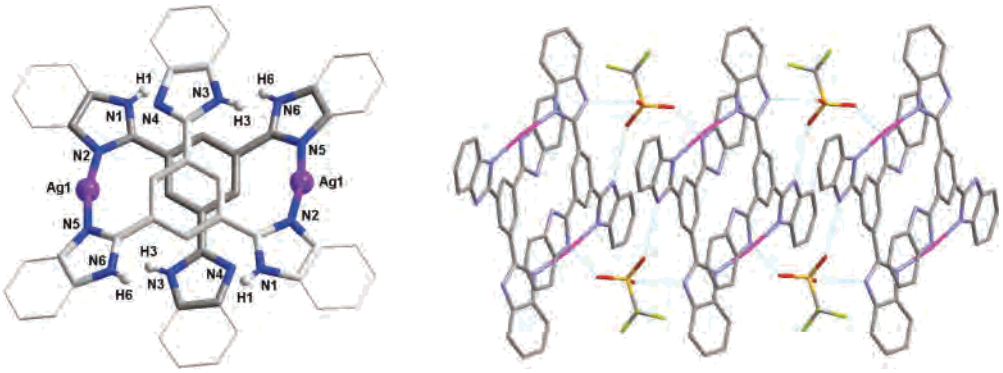

Figure 1. Cationic dimeric structure in complex $[Ag_2(H_3TBimB)_2](CF_3SO_3)_2$ (left) and 1D chain formed via N−H···O hydrogen bonds between dimeric units and the $CF_3SO_3^-$ anions (right).

Scheme 1. H_3TBimB Ligand and Its Stepwise Deprotonated Forms

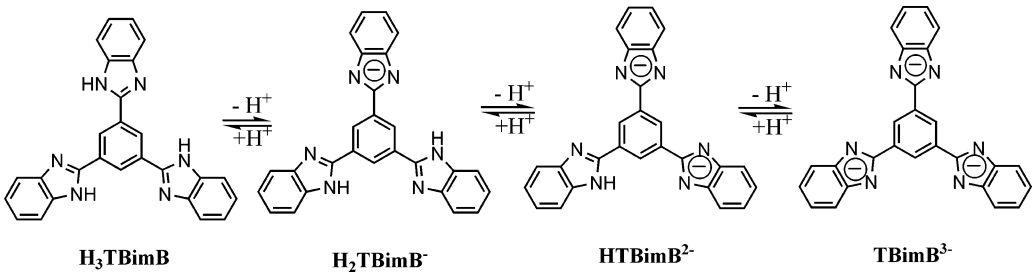

central benzene ring, showing dihedral angles of 23.4, 13.2, and 14.3°, respectively. All amine NH groups are involved in hydrogen-bonding with the $CF_3SO_3^-$ anions (N3−O1, 2.963(6) Å; ∠N3−H3−O1, 173(5)°; N6−O2, 2.885(6) Å; ∠N6−H6−O2, 163(5)°; N1−O3, 2.849(6) Å; ∠N1−H1−O3, 167(6)°). As seen from Figure 1, three O atoms of every $CF_3SO_3^-$ anion form three N−H···O hydrogen bonds with two adjacent dimeric units to join them into a one-dimensional (1D) chain.

$[Ag_4(HTBimB)_2]_n$. In complex **2**, two amine NH groups of each H_3TBimB are deprotonated to give the $HTBimB^{2-}$ dianionic ligand due to the presence of ammonia. The $HTBimB^{2-}$ ligand possesses five potential N coordination donors and one NH hydrogen-bonding donor. However, only four N donors are involved in coordination with the Ag(I) ions while the last one forms a N−H···N hydrogen bond with the NH group from another ligand. Each ligand coordinates with four Ag(I) ions and in turn each Ag(I) ion connects two ligands through Ag−N coordination bonds in a nearly linear coordination geometry (∠N1−Ag1−N4, 176.11(17)° and ∠N5−Ag2−N3, 176.25(17)°). Since every ligand has one N donor and one NH group left, two adjacent ligands form a N−H···N hydrogen bond (N2−N6, 2.617(6) Å; ∠N2−H2A−N6, 174.7°), thus giving rise to a neutral dimeric subunit $[Ag_4(HTBimB)_2]$ as shown in Figure 2a. Different from the dimeric structure in **1**, such dimers are further connected through the external Ag(I) ions and N−H···N hydrogen bonds to result in a 1D coordination polymer (Figure 2c).

It is interesting to compare the present M_4L_2 dimeric unit to the sandwich-shaped M_3L_2 complexes formed from similar triangular disc-shaped ligands 1,3,5-tri(2-benzimidazolyl)-2,4,6-trimethylbenzene and $AgCF_3SO_3$.[7,14] If the external Ag(I) ions are neglected, the dimer in **2** closely resembles the M_3L_2 structures with one Ag(I)−N connection replaced by the N−H···N hydrogen bond. Three benzimidazole arms tilt in the same direction showing dihedral angles of 26.3, 51.5, and 65.3° with respect to the central benzene and lead to a helical arrangement of the dimer. The external Ag(I) ions and N−H···N hydrogen bonds further link such dimers to give a compartmental array (Figure 2b) which is rather similar to the multicompartmental cylindrical nanoarchitectures assembled by Lehn et al.[15] from multicomponent self-assembly of tetrapyridine and hexaphenylhexaazatriphenylene derivated ligands. Moreover, the helical sense of the dimer is homochirally transferred to the neighboring dimers, thus resulting in a helical 1D cylindrical polycompartmental chain. This 1D chain can be regarded as a cylinder surrounded by a triple-stranded helix formed via Ag−N dative-bonding or N−H···N hydrogen-bonding of benzimidazole rings as shown in Figure 2c. In crystal packing, every P helix has three adjacent M helices and vice versa; therefore, the crystal is a racemate containing both right- and left-handed helical chains.

$[Ag_9(HTBimB)_4(TAZ)]_n$. When 1,2,4-triazole (HTAZ) was added in the reaction system of complex **2**, complex **3** was obtained as colorless crystals. The H_3TBimB ligand was changed to $HTBimB^{2-}$ by removal of two protons from the NH groups, just as the case in complex **2**. However, the auxiliary ligand HTAZ was also deprotonated and participated in coordination, thus causing a completely different structural assembly process compared to that of complex **2**.

(14) Hiraoka, S.; Harano, K.; Tanaka, T.; Shiro, M.; Shionoya, M. *Angew. Chem., Int. Ed.* **2003**, *42*, 5182.
(15) Baxter, P. N. W.; Lehn, J.-M.; Kneisel, B. O.; Baum, G.; Fenske, D. *Chem.—Eur. J.* **1999**, *5*, 113.

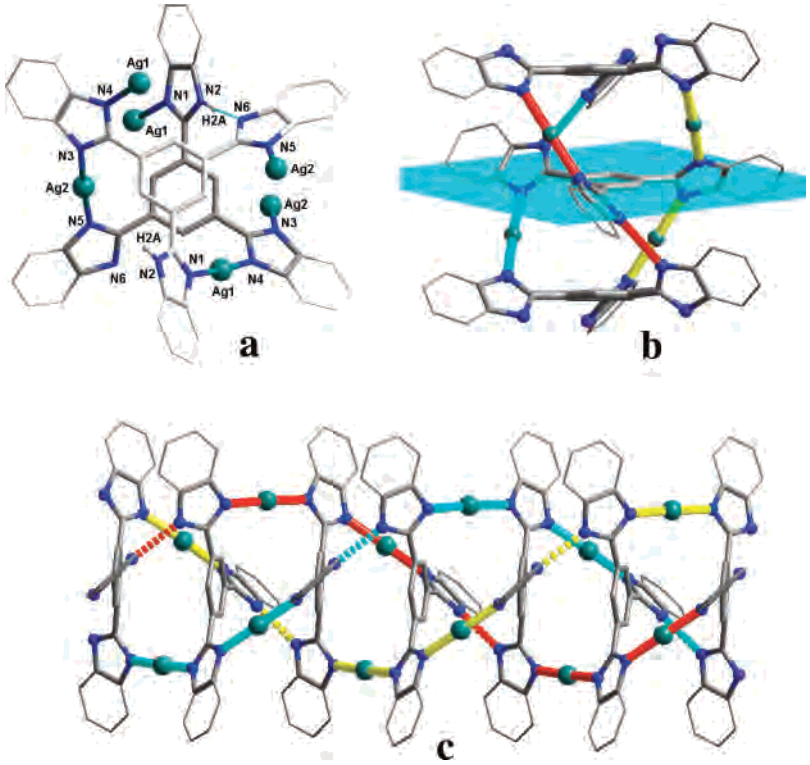

Figure 2. (a) Neutral dimeric unit in complex $[Ag_4(HTBimB)_2]_n$ with N−H···N hydrogen bond shown by a broken line, (b) compartmental array of M_4L_2 dimers, and (c) 1D triple-stranded helical arrangement of benzimidazole arms linked via Ag−N dative bonds and N−H···N hydrogen bonds.

Scheme 2. The Dative-Bonding and Hydrogen-Bonding Modes Exhibited by H_nTBimB Ligands in Complexes **1**−**4**

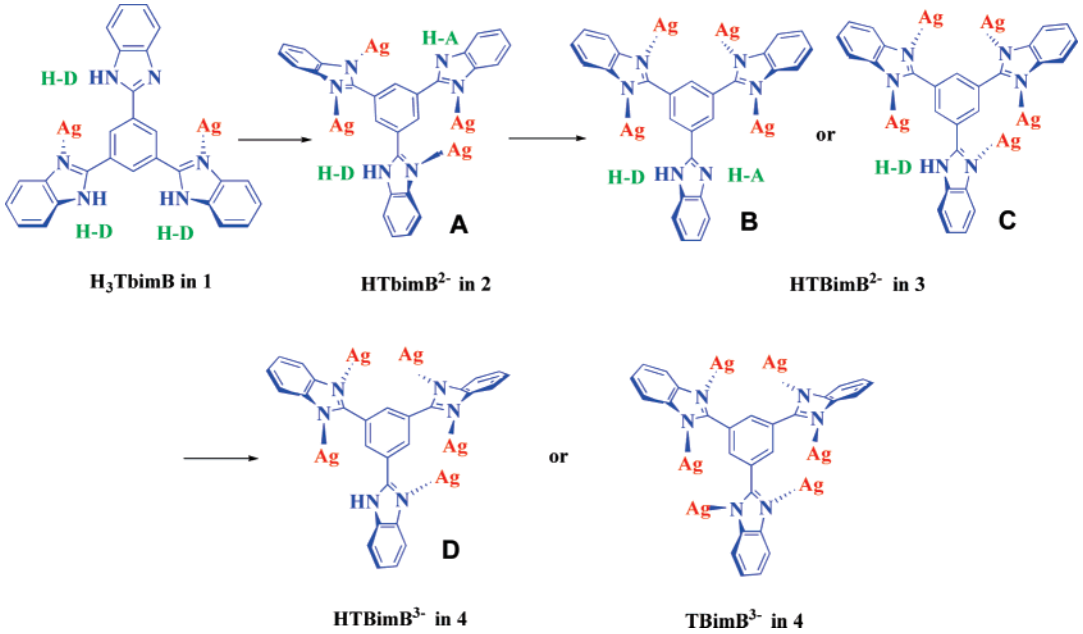

There are two distinguished coordination modes for $HTBimB^{2-}$ (see Scheme 2). In one mode, the $HTBimB^{2-}$ ligand is four dentate, binding to four Ag(I) ions similar to that in complex **2**. While in the other, the $HTBimB^{2-}$ ligand is five dentate coordinating with five Ag(I) ions. Taking the case in complex **2** into consideration, the dianionic $HTBimB^{2-}$ displays three types of distinguishable fashions to interact with the Ag(I) ions as well as to form hydrogen bonds (refer to Scheme 2): (a) a four dative-bonding and two hydrogen-bonding mode (mode A). One deprotonated benzimidazole arm connects two Ag(I) ions; the other deprotonated arm connects one Ag(I) ion with the uncoordinating N atom acting as the hydrogen-bonding acceptor, while the non-deprotonated arm connects one Ag(I) ion with the NH group acting as a hydrogen-bonding donor. (b) A second distinguishable fashion is a similar four dative-bonding and two hydrogen-bonding mode (mode B) as shown in Scheme 2. Both two deprotonated arms connect two Ag(I) ions while the nondeprotonated arm offers one N atom as a hydrogen-bonding acceptor and one NH group as a hydrogen-bonding

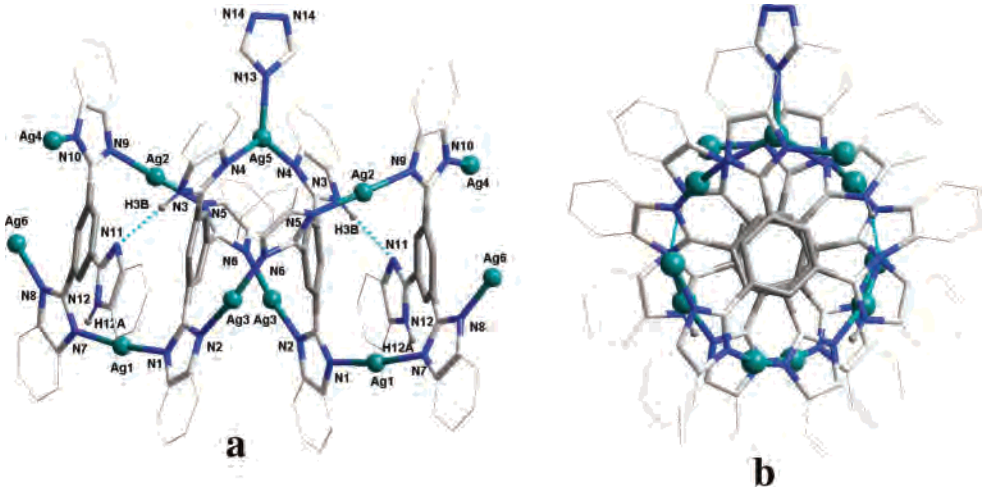

Figure 3. (a) Neutral oligonuclear $[Ag_9(HTBimB)_4(TAZ)]$ structural unit in complex **3** with N−H···N hydrogen bonds shown by broken lines and (b) top view of the basic unit showing wrapping of the benzimidazole rings around the central benzene rings.

donor. (c) A third distingushable fashion is a five dative-bonding and one hydrogen-bonding mode (mode C) as shown in Scheme 2. All five N atoms in three benzimidazole arms connect Ag(I) ions while the remaining NH group acts as a hydrogen-bonding donor.

Single-crystal X-ray diffraction analysis reveals that the asymmetric unit contains two $HTBimB^{2-}$ dianions, half a TAZ^- anion, three crystallographically independent Ag(I) ions, and three half-occupied Ag(I) ions. Therefore, the basic structural unit of complex **3** can be considered as $[Ag_9(HTBimB)_4(TAZ)]$ which possesses a 2-fold symmetry bisecting the TAZ^- anion as shown in Figure 3. The Ag(I) ions display two different coordination geometries: one is linearly two-coordinated and the other is triangularly three-coordinated. The TAZ^- anion behaves as a monodentate ligand to complete the triangular coordination geometry of one Ag(I) ion, but the remaining two N atoms are free of complexation. Alternatively, they behave as hydrogen-bonding acceptors which will be discussed later. As shown in Figure 3, the $[Ag_9(HTBimB)_4(TAZ)]$ subunit exhibits a helical sense with benzimidazole arms wrapping around the central benzene rings and connected through Ag(I) ions in between every two ligands. Two N−H···N hydrogen bonds are formed between uncoordinated N atoms and the NH groups (N3−N11, 2.954(14) Å; ∠N3−H3B−N11, 169.6°). Therefore, the triple-stranded helical arrangement of the benzimidazole rings which are Ag−N dative-bonded or N−H···N hydrogen-bonded is observed, similar to that in complex **2**.

Since the TAZ^- anion is not a bridging ligand, the $[Ag_9(HTBimB)_4(TAZ)]$ subunit may be simplified as an M_9L_4 motif, which also has four external Ag(I) ions ready for connecting the neighboring units. In contrast to the M_4L_2 subunit in complex **2**, the four external Ag(I) ions in M_9L_4 unit join four different units in four directions to generate a two-dimensional (2D) network, rather than a 1D polymeric chain as in **2**. When the M_9L_4 subunit is regarded as a four connecting node, the 2D network can be reduced to a (4,4) topological net.[3a,16] As shown in Figure 4a, the 2D network is actually sustained by Ag−N bonds. If the central benzene rings are neglected and only connectivity between the benzimidazole rings is considered, it is clear that the two Ag−N dative-bonding strands of the helical M_9L_4 motif are not extended in the same direction to keep the helical sense but crossly entangled to weave a sheet which is represented in Figure 4b. In addition, the third strand of the helical M_9L_4 motif, comprising Ag−N bonds and N−H···N hydrogen bonds, threads through the 2D entanglement and extends as a single helix. On the basis of this single helix, the M_9L_4 subunits are strung together to form a 1D chain (Figure 4c), and the 2D network can also be considered to be generated from the cross-linking of such 1D chains. It should be noticed that extension of this single helix involves the N−H···N hydrogen bonds (N12−N14, 2.780(16) Å; ∠N12−H12A−N14, 159.6°) formed between TAZ^- and the NH groups of the benzimidazole ring as shown in Figure 4c. By utilization of these types of hydrogen bonds, these 1D chains can also be connected into the 2D network of the same (4,4) topology as depicted in Figure 4d.

$[Ag_{17}(TBimB)_5(HTBimB)(H_2O)_5]_n \cdot n(H_2O)$. Complex **4** was confirmed by single-crystal analysis as a 3D framework. Each asymmetrical unit is composed of three ligands, three water molecules, and eight and one-half Ag(I) ions. Figure 5a shows the arrangement of three ligands and the coordination geometry of every Ag(I) ion. It is clear that the H_3TBimB ligand was changed to two different forms: one is fully deprotonated to become the six dentate $TBimB^{3-}$ trianion and the other is partially deprotonated to give the five dentate $HTBimB^{2-}$ dianion. The $HTBimB^{2-}$ dianion displays the same coordination mode as mode C (Scheme 2) in complex **2**; however, the remaining NH group in this case does not form any hydrogen bond, thus providing the fourth fashion (mode D in Scheme 2) in construction of Ag(I) complexes. The Ag(I) ions adopt four differentiable coordination geometries: Ag(1) coordinates with three N donors from three different ligands to form a trigonal environment; Ag(2) and Ag(3) are also triangularly coordinated but to two N donors from two different ligands and

(16) Chen, C.-L.; Goforth, A. M.; Smith, M. D.; Su, C.-Y.; zur Loye, H.-C. *Inorg. Chem.* **2005**, *44*, 8726.

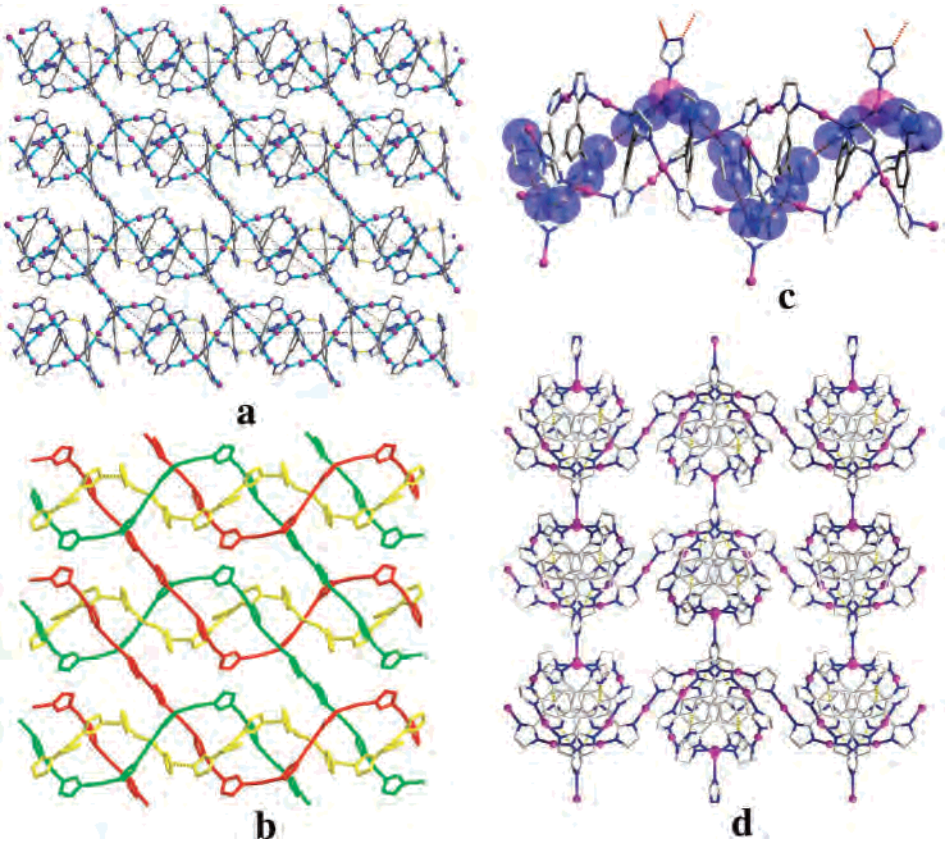

Figure 4. (a) 2D network sustained by Ag−N dative bonds (highlighted in cyan) in complex **3** showing (4,4) topology (represented by gray dashed lines) with the benzimidazole ring simplified as an imdazole ring for clarity, (b) connectivity between the imidazole rings through Ag−N bonds and N−H···N hydrogen bonds (shown in broken lines) with all benzene rings omitted for clarity, (c) 1D chain formed via connecting M_9L_4 subunits by the single helix (represented in space-filling mode) which itself extends through the Ag−N dative- and N−H···N hydrogen-bonding (shown in broken lines), and (d) 2D (4,4) network formed via hydrogen-bonding of 1D chains through TAZ^- ligands in the *bc* plane.

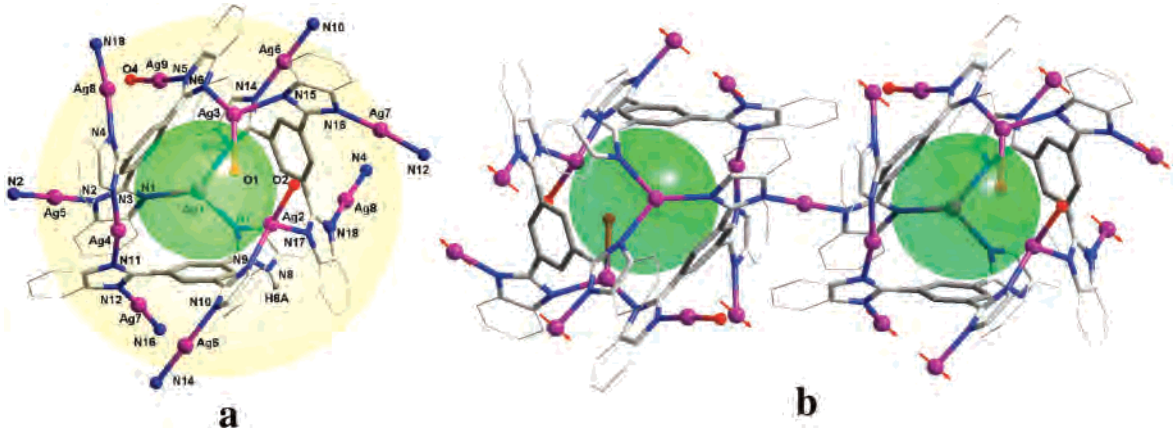

Figure 5. (a) Molecular structure in the asymmetric unit in complex **4** showing coordination geometry of every Ag(I) ions and M_4L_3 cage demonstrated by fitting a transparent green ball inside. (b) The $[Ag_{17}(TBimB)_5(HTBimB)(H_2O)_5]$ subunit composed of two C_2-symmetry related M_4L_3 cages with 12 external Ag(I) ions showing atom vectors directed toward neighboring units.

one O donor from the water molecule; Ag(9) is a little unusual, connecting one N donor and one aqua O donor; all other Ag(I) ions link two N donors of two different ligands leading to the linear coordination environment. Since the Ag(5) ion is located on a 2-fold axis thus half occupied, the basic structural unit in complex **4** can be described as a 17-nuclear $[Ag_{17}(TBimB)_5(HTBimB)(H_2O)_5]$ motif possessing inner C_2 symmetry as shown in Figure 5b. Such crystallographically imposed symmetry requires that the two halves of the $[Ag_{17}(TBimB)_5(HTBimB)(H_2O)_5]$ unit are strictly equivalent; thus, the proton of $HTBimB^{2-}$ dianion and one water molecule have to be shared, and therefore, half fractional refinement of the proton and one coordinated water molecule were applied in the structural analysis.

It is interesting that molecular structure in the asymmetric unit exhibits an open-faced M_4L_3 cage (Figures 5a and 6a), analogous to the Ag_4L_4 cage structure reported by Shionoya et al.[7] One face of the tetrahedral M_4L_4 cage is missing with two Ag(I) ions bonding two water molecules and one Ag(I) ion being only two-coordinated. Two such cage motifs are

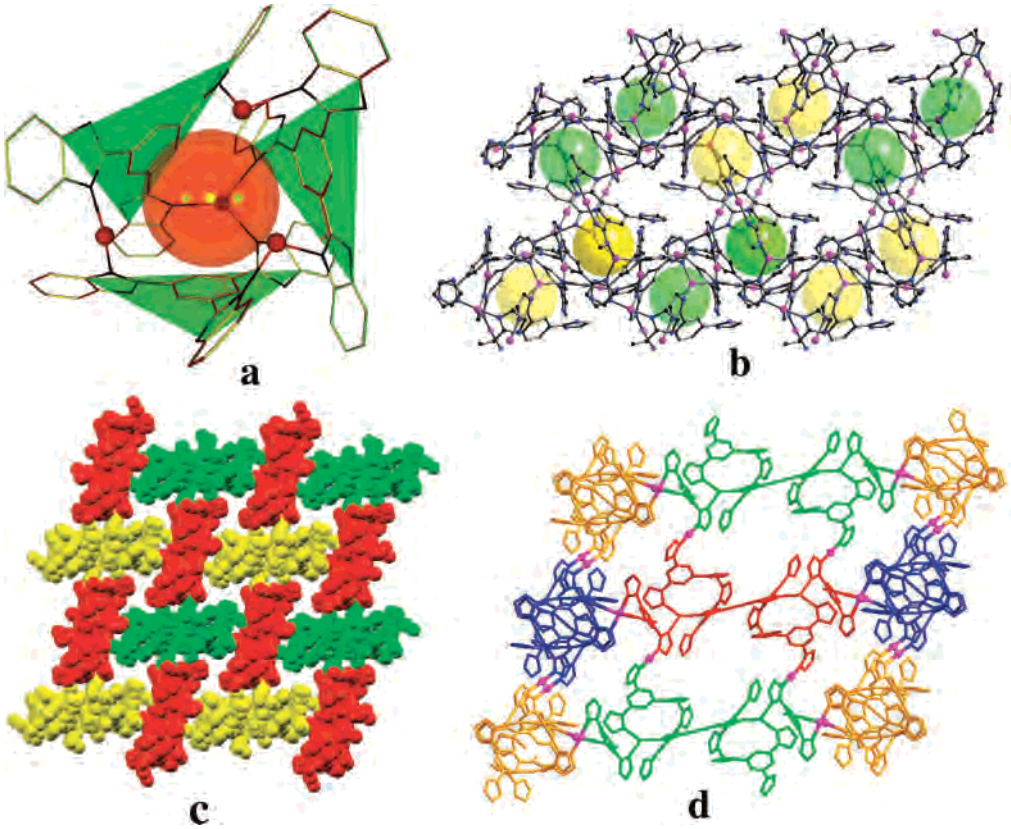

Figure 6. (a) The open-faced M_4L_3 in **4** showing three closed faces with green triangles and an inner cavity with a red ball, (b) 3D framework constructed by the double-cage $M_{17}L_6$ subunits (in ball−stick mode), (c) 2D network formed in the $(01\bar{1})$ plane with every subunit connecting four neighbors (in space-filling mode), and (d) 2D network formed in the (101) plane showing connections via external Ag(I) ions (mauve ball) between subunits (in stick mode). The benzimidazole rings are simplified as imdazole rings for clarity in parts c and d.

bridged via Ag(5) to offer the double-cage subunit (Figure 5b), which possesses 12 external Ag(I) ions to interact with the neighboring subunits. Because the water molecules are only served as auxiliary ligands to complete the coordination geometry of Ag(I) ions, the oligonuclear $[Ag_{17}(TBimB)_5(HTBimB)(H_2O)_5]$ structural units can be simplified as a $M_{17}L_6$ motif. Detailed structural analysis revealed that the 12 Ag(I) ions compose six pairs of connections directing to six adjacent $M_{17}L_6$ subunits, thus generating a three-dimensional (3D) framework as depicted in Figure 6b. To analyze this in a simple way, the 2D network can be considered to be generated in the $(01\bar{1})$ plane by four pairs of Ag−N connections which join four adjacent subunits as shown in Figure 6c, while in the (101) plane, a similar 2D network is formed with each subunit connected with four neighbors. Since both the 2D networks formed in two noncoplanar directions are of (4,4) topology and each $M_{17}L_6$ structural unit is six-connected, the overall 3D framework can be described as a cubic net.[3a,17] The open-faced M_4L_3 cages contain a cavity which is estimated by the program Platon[18] to have an effective volume of 75 Å^3; thus, the 3D framework displays a slight porosity due to such polycage character.[18] Calculation using the program Platon indicates an effective solvent accessible volume of 818 Å^3, comprising 10.5% of the unit cell for inclusion of solvent molecules. Structural analysis indeed confirms that solvated water molecules are hosted inside the lattice cavities.

Structural Comparison. We have intended to remove three protons from the H_3TBimB ligand step by step under controllable reaction conditions and hope to obtain Ag(I) complexes with successively deprotonated ligands. However, this was proven difficult because the reaction mechanism under the black-boxlike solvothermal conditions[6c] is largely unknown and various influencing factors including pH value adjustment are quite different from ordinary conditions. Therefore, precise conditions of the reaction are actually beyond control. Nevertheless, Ag(I) complexes of the non-deprotonated, dideprotonated, and trideprotonated ligands have been obtained, in which ligands display diversified coordination modes as well hydrogen-bonding fashions as depicted in Scheme 2.

The nonprotonated H_3TBimB ligand forms a 0D Ag_2L_2 dinuclear structure in complex **1** which is connected by the $CF_3SO_3^-$ anion via N−H···O hydrogen bonds to give a 1D chain. In the presence of ammonia, the H_3TBimB ligand is deprotonated to offer a $HTBimB^{2-}$ dianion. Reaction of this dianion with Ag(I) ion in a 25% ammonia system results in a polycompartmental 1D coordination polymer in complex **2,** which consists of Ag_4L_2 building units extended via Ag−N dative-bonding and N−H···N hydrogen-bonding in a triple-stranded helical way. The same reaction of $HTBimB^{2-}$

(17) (a) Su, C.-Y.; Kang, B.-S.; Yang, Q.-C.; Mak, T. C. W. *J. Chem. Soc., Dalton Trans.* **2000**, 1831. (b) Su, C.-Y.; Kang, B.-S.; Yang, Q.-C.; Mak, T. C. W. *J. Chem. Soc., Dalton Trans.* **2000**, 1857. (c) Su, C.-Y.; Yang, X.-P.; Kang, B.-S.; Mak, T. C. W. *Angew. Chem., Int. Ed.* **2001**, *40*, 1725.

(18) Spek, A. L. *Acta Crystallogr., Sect. A* **1990**, *46*, C34.

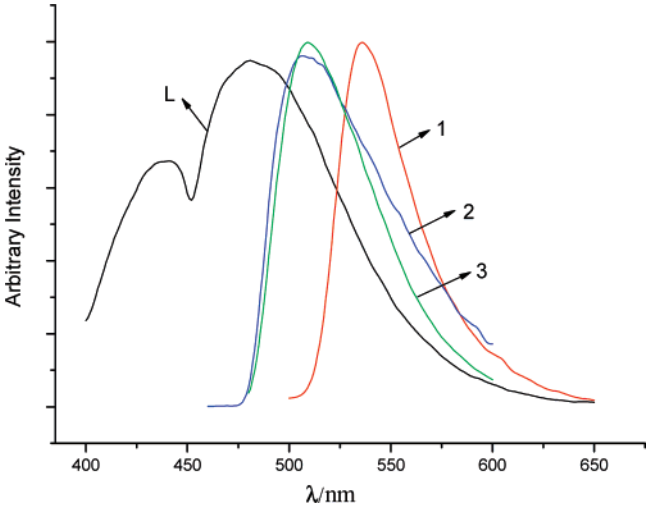

Figure 7. Emission spectra of complexes **1**−**3** and ligand H_3TBimB in the solid state at room temperature.

dianion and Ag(I) ion in the presence of an auxiliary HTAZ ligand leads to formation of a 2D network in complex **3**. The dianions exhibit two different coordination modes to result in an M_9L_4 subunit with benzimidazole rings linked via Ag−N bonds and N−H···N hydrogen bonds to show a similar triple-stranded helical arrangement as in **2**. However, two dative-binding helical strands are extended in a crossly entangled way to weave the 2D sheet. When Bu_4NBr was added into the reaction system of **2**, the 3D framework is generated with part of the $HTBimB^{2-}$ further deprotonated to give $TBimB^{3-}$ trianion in complex **4**. The trianions interact with Ag(I) ions together with the $HTBimB^{2-}$ dianions to give rise to an $M_{17}L_6$ structural unit which contains two M_4L_3 open-faced cages. Therefore, the 3D framework is a polycage structure showing 10.5% porosity and hosting water guest molecules.

Property Study. Powder X-ray diffraction (XRD) has been used to check the phase purity of the bulky samples in the solid state. For complexes **1**−**3**, the measured XRD patterns closely match the simulated patterns generated from the results of single-crystal diffraction data (Supporting Information, Figure S2), indicative of pure products. However, no satisfactory XRD pattern was obtained for complex **4**. The thermogravimetric analysis (TGA) was performed in air on a polycrystalline sample of complex **2**. The TGA diagram (Supporting Information, Figure S1) shows only one step of decomposition in the temperature range 23−700 °C. The weight loss occurred at about 500 °C and lost most of the organic component in an abrupt stage. The photoluminescence property of the ligand H_3TBimB and complexes **1**−**3** was investigated in the solid state. As shown in Figure 7, the nondeprotonated ligand displays two emission peaks around 438 and 480 nm. After coordination, only one emission peak appears. The strongest emissions were found at 536 nm (λ_{ex} = 485 nm) for complex **1** and at 505 and 508 nm (λ_{ex} = 448 nm) for complexes **2** and **3**, respectively, all showing significant red-shift compared to that of the ligand. It is a surprise that the maximum of the emission band of complex **1** shows more red-shift than those of complexes **2** and **3**, indicating that emissions in these complexes include ligand-to-metal charge transfer (LMCT) character.[20] The different nature of the nonprotonated and diprotonated ligands as well as their different coordination behaviors may be the reason the emission bands are shifted to different extents.

Conclusion

A systematic study of the coordination behavior toward the Ag(I) ion has been carried out for the rigid triangular ligand 1,3,5-tri(2-benzimidazolyl)benzene and its deprotonated forms (H_nTBimB^m, n = 3, 1, 0 and m = 0, −2, −3, respectively) under solvothermal conditions. Generally speaking, the H_3TBimB ligand and its deprotonated forms provide diversified coordination modes and hydrogen-bonding fashions in complexes **1**−**4**: H_3TBimB is three-dentate and triply hydrogen-bonded, $TBimB^{3-}$ trianion is six-dentate, while the $HTBimB^{2-}$ dianion is versatile to act as four- or five-dentate and both a hydrogen-bonding donor or an acceptor ligand, in four totally distinguishable modes. Along with removal of more protons, and more N donor atoms and negative charges becoming available, larger oligonuclear Ag(I) building units are aggregated, thus resulting in the dimensional increase of Ag(I) coordination assemblies from 0D to 3D. Taking into consideration the unknown H_2TBimB^- anion and other varied potential coordination modes of H_nTBimB^{m-}, even diversified structures and topologies can be expected for their Ag(I) complexes. Further investigation is now underway.

Acknowledgment. This work was supported by the National Science Funds for Distinguished Young Scholars of China (Grant 20525310), the NSF of China (Grant 20673147), Guangdong Province (Grant 04205405), and RFDP of the Education Ministry of China.

Supporting Information Available: X-ray crystallographic data (CIF format), TGA curve of complex **2**, and XRD patterns for complexes **1**−**3**. This material is available free of charge via the Internet at http://pubs.acs.org.

IC070309K

(19) Lu, W.-G.; Su, C. Y.; Lu, T.-B.; Jiang, L.; Chen, J.-M. *J. Am. Chem. Soc.* **2006**, *128*, 34.

(20) (a) Liu, S. Q.; Kuroda-Sowa, T.; Konaka, H.; Suenaga, Y.; Maekawa, M.; Mizutani, Y.; Ning, G. L.; Munakata, M. *Inorg. Chem.* **2005**, *44*, 1031. (b) Han, L.; Yuan, D. Q.; Xu, Y. Q.; Wu, M. Y.; Gong, Y. Q.; Wu, B. L.; Hong, M. C. *Inorg. Chem. Commun.* **2005**, *8*, 529. (c) Valencia, L.; Bastida, R.; Macías, A.; Vicente, M.; Lourido, P. P. *New J. Chem.* **2005**, *29*, 424. (d) Wang, Y.; Yi, L.; Yang, X.; Ding, B.; Cheng, P.; Liao, D.-Z.; Yan, S. P. *Inorg. Chem.* **2006**, *45*, 5822. (e) Xia, C. K.; Lu, C. Z.; Zhang, Q. Z.; He, X.; Zhang, J. J.; Wu, D. M. *Cryst. Growth Des.* **2005**, *5*, 1569.